

# A direct fluorescence-based technique for cellular localization of amylin

Karen Pillay  
Patrick Govender\*

School of Life Sciences, University of KwaZulu-Natal, South Africa

## Abstract

Amylin has been implicated in type II diabetes because of its inherent property to misfold into toxic aggregates. Although it has been shown that amylin interacts with cell membranes, no study to date has monitored the association process using a direct approach. The present study uses confocal microscopy to identify the localization of carboxyfluorescein-labeled amylin in RIN-5F cells. In addition, the size of the aggregates

that are formed was evaluated using nanoparticle tracking analysis. In support of previous findings, amylin was observed to interact with and remain associated with the cell membrane. The cell membrane-associated aggregates spanned a size range of 130–800 nm. © 2013 International Union of Biochemistry and Molecular Biology, Inc. Volume 60, Number 4, Pages 384–392, 2013

**Keywords:** amylin, carboxyfluorescein, RIN-5F, type II diabetes

## 1. Introduction

Misfolding of peptides or proteins into toxic oligomers and fibrils results in a number of diseases collectively classified as amyloid diseases [1–5]. Of these, type II diabetes and Alzheimer's disease are currently the most prevalent in society [5]. In type II diabetes, the peptide that is implicated in disease progression is amylin, which is also referred to as islet amyloid polypeptide [1–3, 6]. Amylin is composed of 37 amino acids with a disulfide bridge between residues 2 and 7 (Fig. 1) and aggregates into oligomers that are in a  $\beta$ -sheet conformation and that are toxic to pancreatic *beta* cells [1–3, 7–13]. Although there has been extensive research on potential inhibitors of amylin-mediated cytotoxicity, most of these studies have

interrogated molecules that bind to amylin, which subsequently inhibits fibrillogenesis [10, 13–31]. However, to the best of our knowledge, there is currently no inhibitor of amylin aggregation that is a potential therapeutic agent for type II diabetes and that is under consideration for clinical development [32]. In an attempt to unravel its cellular pathway, it would be strategically beneficial to map the cellular localization of amylin aggregates so as to affect the design of inhibitors of amylin aggregation and toxicity.

Initial studies on amylin localization employed immunogold labeling and showed that amylin is present in lipofuscin bodies in pancreatic *beta* cells of diabetic patients [6]. Subsequent studies suggested that amylin lies in close proximity to the external cell surfaces, namely the cell membrane and islet capillaries [33–39]. However, none of these studies evaluated amylin localization in an *in vitro* mammalian cell-based system.

The study herein attempts to describe the real time *in vitro* cellular tracking of carboxyfluorescein-labeled amylin (carboxy-amy) aggregates in the rat pancreatic *beta* (RIN-5F) cell line. This cell line was selected as it represents the *in vivo* cytotoxic target of amylin aggregates and thus observations could provide an insight as to what occurs in the biological scenario. The advantages of the proposed strategy are that it employs direct visualization of amylin localization and hence precludes the use of multiple labeling steps and also limits the possibility of nonspecific interactions. Nanoparticle tracking analysis (NTA) was also performed to concisely estimate the size of amylin aggregates that are formed.

Most studies until now have incorporated an indirect labeling approach using Congo red to distinguish amylin aggregates or used other dyes to identify cellular components

---

**Abbreviations:** carboxy-amy, carboxyfluorescein-labeled amylin; DIPEA, *N,N*-diisopropylethylamine; DMF, dimethyl formamide; Fmoc, 9-fluorenylmethoxycarbonyl; GUVs, giant unilamellar vesicles; HFIP, hexafluoroisopropanol; HPLC, high-performance liquid chromatography; MALDI-TOF MS, matrix-assisted laser desorption ionization time-of-flight mass spectroscopy; MS, mass spectra; NTA, nanoparticle tracking analysis; RIN, rat insulinoma tumor cell line; *t*Bu, *t*-butyl ether; TEM, transmission electron microscopy; TFA, trifluoroacetic acid.

\*Address for correspondence: Patrick Govender, PhD, University of KwaZulu-Natal, Westville Campus, Block F3, Department of Biochemistry, University Road, Private Bag X54001, Durban 4000, South Africa. Tel.: +27 31 260 7814/7665; Fax: +27 31 260 7942; e-mail: govenderpt@ukzn.ac.za.

Received 11 December 2012; accepted 11 March 2013

DOI: 10.1002/bab.1113

Published online 21 August 2013 in Wiley Online Library (wileyonlinelibrary.com)



with *N*-[(dimethylamino)-1*H*-1,2,3-triazolo[4,5-*b*]pyridino-1-ylmethylene]-*N*-methylmethanaminium hexafluorophosphate *N*-oxide and DIPEA in DMF serving as the activator and activator base, respectively. The peptide was subsequently cleaved from the resin using 5% tri-isopropylsilane in trifluoroacetic acid (TFA) for 2 H. Chemically synthesized human amylin (amylin) was used as the control for transmission electron microscopy (TEM) and NTA [52].

### 2.3. Peptide purification

Carboxy-amy was purified on an ACE C18 preparative column (250 × 22 mm<sup>2</sup>; Scotland) as previously described [52]. A dual-buffer system was employed, with TFA serving as the ion-pairing agent. The first buffer consisted of 0.1% TFA/H<sub>2</sub>O (v/v), and the second buffer contained 0.1% TFA/acetonitrile (v/v). The peptides were eluted using a gradient of 0%–90% buffer B over 90 Min with a flow rate of 20 mL/min. The solvent from pooled peptide-containing fractions was evaporated to 20 mL, and the samples were snap-frozen in liquid nitrogen and lyophilized.

### 2.4. Peptide analysis

The purified peptide was analyzed with an Agilent 1100 HPLC system fitted with a Waters XBridge C18 column, 250 × 3.6 mm<sup>2</sup> as previously described [52]. Chromatography was performed over 90 Min using a gradient of 0%–90% buffer B at a flow rate of 0.3 mL/min, and the eluent was monitored at a UV wavelength of 215 nm. A Bruker electrospray ionization time-of-flight spectrometer in positive mode was used to obtain mass spectra (MS) and matrix-assisted laser desorption ionization time-of-flight mass spectroscopy (MALDI-TOF MS) was performed with an Autoflex III instrument (Bruker, Germany) operated in positive mode with cyano-4-hydroxycinnamic acid being used as the matrix.

### 2.5. Disaggregation method

Disaggregation of carboxy-amy was performed as previously described [52]. Preweighed amylin samples were solubilized in 200 μL hexafluoroisopropanol (HFIP)–TFA solution (50:50, v/v), sonicated for 10 Min and left overnight. The solvents were then removed under vacuum using a centrifugal evaporator for approximately 1–2 H. Approximately 100 μL HFIP was added to the amylin, followed by vortexing and the solvent was removed by rotary evaporation for 1–2 H. To remove all traces of TFA, the latter process was repeated twice using HFIP (100 μL).

### 2.6. TEM

Carboxy-amy and amylin were disaggregated as described above and dissolved in filter sterilized 10 mM sodium phosphate buffer, pH 7.4, containing 50 mM NaCl (Buffer A) to a final concentration of 30 μM. Samples were incubated at 37 °C and at specific time points 2 μL aliquots of each sample were transferred onto formvar-coated carbon-stabilized copper grids. After drying for 1 Min, excess liquid was blot dried and samples were stained with 2% (w/v) uranyl acetate for 30 Sec. Samples were blot dried again before being analyzed with a

CM120 Biotwin Philips transmission electron microscope at a voltage of 100 V.

### 2.7. Confocal microscopy

The RIN-5F cell line (European Collection of Cell Cultures; Sigma–Aldrich) was cultured in RPMI 1640 growth medium containing 10% heat-inactivated fetal bovine serum, 2 mM glutamine, 1 mM sodium pyruvate, 25 mM 2-[4-(2-hydroxyethyl)-1-piperazinyl] ethanesulfonic acid, and 0.1 mg/mL penicillin/streptomycin and thereafter plated at a density of  $4 \times 10^4$  cells into 35 mm glass bottom petri dishes containing 14 mm micro wells (kindly donated by Dr. Celia Snyman, University of KwaZulu-Natal). After an incubation period of 24 H at 37 °C, spent medium was replaced with fresh medium. To establish whether carboxyfluorescein was susceptible to photo bleaching effects, carboxyfluorescein only (2.54 μM, equivalent to the amount of carboxyfluorescein present in 30 μM of carboxy-amy) was added to the RIN-5F cells and monitored over time. Images were viewed and captured with a Zeiss 710 laser-scanning confocal microscope and Zeiss LSM 710 software at 10 Min intervals for the first hour and then every 30 Min until 3 H, using a 63× oil immersion objective. Twelve slices at different focal points were captured at each interval. A 488 nm argon laser was used for excitation of the fluorophore, whereas emission was captured at 520 nm. Images were also simultaneously captured using differential interference contrast (DIC) microscopy. To track the cellular localization of carboxy-amy, RIN-5F cells were grown and plated as described above. After an incubation period of 24 H, spent medium was removed and carboxy-amy was dissolved in growth medium and added to the cells to a final concentration of 30 μM. At the end of the experiment, growth medium was recovered from the samples and later analyzed using NTA. All experiments were performed in duplicate with the temperature of the sample chamber set to 37 °C.

### 2.8. NTA

NTA measurements were performed with a NanoSight LM20 instrument (NanoSight, Amesbury, UK) equipped with a 488 nm laser for exciting the carboxyfluorescein tag and a temperature-controlled sample chamber set at 37 °C. To establish whether the carboxyfluorescein tag aggregates on its own, carboxyfluorescein only (2.54 μM, equivalent to the amount of carboxyfluorescein present in 30 μM of carboxy-amy) was prepared in Buffer A and NTA performed by recording 60 Sec videos with the single shutter and gain modes. An analysis was performed using NanoSight NTA 2.2 software with a viscosity setting of 0.70. Samples recovered from confocal microscopy experiments were captured and analyzed using NTA as described above. To monitor the aggregation dynamics of carboxy-amy over time, disaggregated peptide was diluted in Buffer A and sonicated for 5 Min to yield a concentration of 30 μM before being injected into the sample chamber. Sample temperatures were allowed to equilibrate to 37 °C (approximately 1 Min) before 60 Sec video recordings were taken at specific time

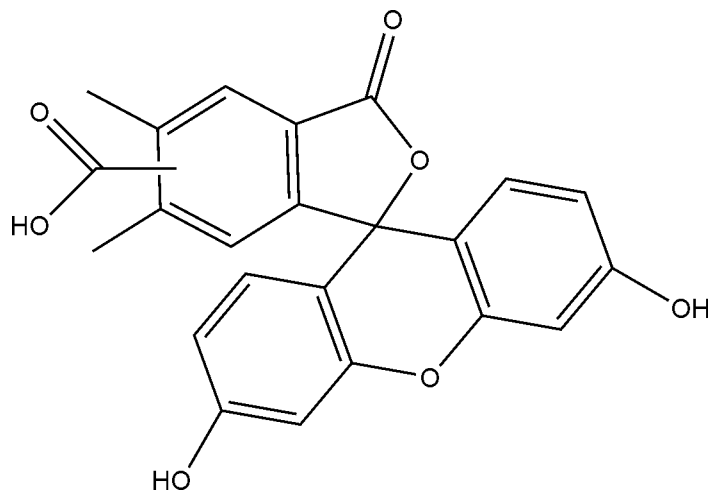


**FIG. 2** Structure of 5(6)-carboxyfluorescein.

points (every 10 Min for the first hour and then every 30 Min until 3 H). Videos were captured and analysis performed as described above.

### 3. Results

In developing a suitable fluorescence strategy that will enable real-time tracking of the interaction of amylin aggregates with cellular components, it was deemed critical that the chemical modification must not interfere with its amyloidogenic potential. In this regard, the N-terminal lysine residue was selected as a suitable site of attachment of the fluorophore as there is general agreement that the N-terminal region of amylin is not involved in amylin fibril formation [53, 54]. Carboxyfluorescein was chosen as a suitable fluorophore as it was previously reported that a fluorescein label at the N-terminal of full-length amylin [21] or on amyloid *beta*, the amyloidogenic peptide responsible for Alzheimer's disease, had no significant effect on the amyloidogenic properties of these peptides [53, 54]. Moreover, some of the advantages that are associated with the use of carboxyfluorescein (Fig. 2) are its high molar absorptivity, excellent fluorescence quantum yield, good solubility in water, and an excitation of 494 nm, close to the 488 nm spectral line of the argon laser, which makes it suitable for confocal microscopy imaging [55]. As illustrated in Fig. 3, carboxy-amy was synthesized with high purity and a yield of 8% (34 mg).

As ascertained by TEM analysis, amylin fibrils emanating from carboxy-amy exhibited a similar morphology to fibrils formed by unmodified amylin (Fig. 4).

Confocal microscopy imaging analysis confirmed that the carboxyfluorescein fluorophore was stable over the experimental duration, in that no photobleaching was evident as the intensity of the fluorescent signal was not reduced (Fig. 5).

Analysis of confocal microscopy generated images seems to suggest that aggregates of carboxy-amy that are indicated

by colored (yellow, white, blue, red, and pink) arrows strongly interact with the extracellular face of the RIN-5F plasma membrane (Fig. 6). This is shown by aggregates remaining associated with the plasma membrane, although the cellular morphology in certain instances changes markedly over the 3 H duration of the experiment. It is noteworthy that carboxy-amy cannot be observed intracellularly.

NTA of samples containing only carboxyfluorescein illustrated a background fluorescence without any discernible aggregates being observed at all time points. The presence of a faint background indicates that the fluorophore is present but does not form aggregates greater than 30 nm in size and thus cannot be detected as the size range for NTA is 30–1,000 nm [56].

During NTA, resuspension, injection, and equilibration times resulted in a time lapse of approximately 10 Min, thereby rendering analysis of a zero time point impractical. As can be seen in Fig. 7 (graph A), the predominant size of carboxy-amy at the 10 Min time point is between 40 and 90 nm, reaching a concentration greater than  $2 \times 10^7$  aggregates/mL. Other peaks represented aggregates that were in the size range 90–260 nm that occurred at concentrations between  $0.5 \times 10^7$  aggregates/mL and  $1 \times 10^7$  aggregates/mL. In addition, another predominant peak represented an aggregate cohort with a size of approximately 510 nm and concentration of approximately  $0.7 \times 10^7$  aggregates/mL. After 3 H (Fig. 7, graph B), the concentration of 100–170 nm aggregates was below  $0.5 \times 10^7$  aggregates/mL, whereas the predominant peaks representing aggregates in the 170–250 and 250–360 nm ranges were present at concentrations above  $1 \times 10^7$  aggregates/mL, indicating that the smaller sized aggregates (40–90 and 90–170 nm) that were present at the 10 Min time point have now grown into larger particles (170–250 and 250–360 nm). Interestingly, the observed 510 nm peak at the 10 Min interval is not evident after 3 H. Rather, the emergence of two new peaks (360–520 and 640–850 nm) is observed. Growth medium that was recovered from the confocal microscopy experiment (Fig. 7, graph C) and that was subjected to NTA revealed a carboxy-amy aggregate size distribution profile that was similar to that of the carboxy-amy sample alone after an incubation period of 3 H (Fig. 7, graph B). However, a higher concentration of particles in all size ranges except the 270–400 nm range was observed in the sample recovered from the confocal microscopy experiment.

### 4. Discussion

As mentioned previously, it is widely accepted that the aggregated form of amylin is linked to the destruction of pancreatic *beta* cells. It is therefore prudent that technology is developed that provides a closer insight into the interaction of amylin aggregates with cellular structures. This awareness may in part contribute to the successful design of an effective inhibitor of amylin aggregation. Until now the cellular tracking of amylin aggregates has been reliant on indirect labeling

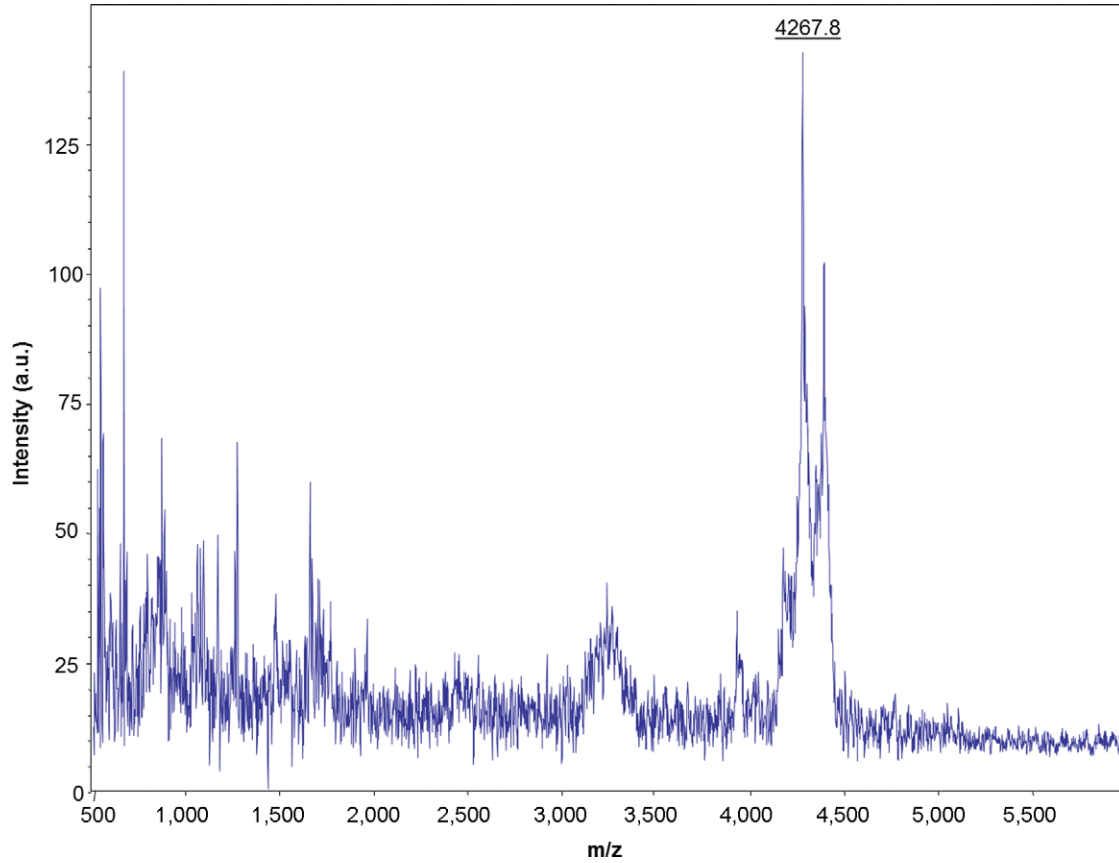


**FIG. 3** MALDI-TOF spectrum of chemically synthesized carboxy-amy.

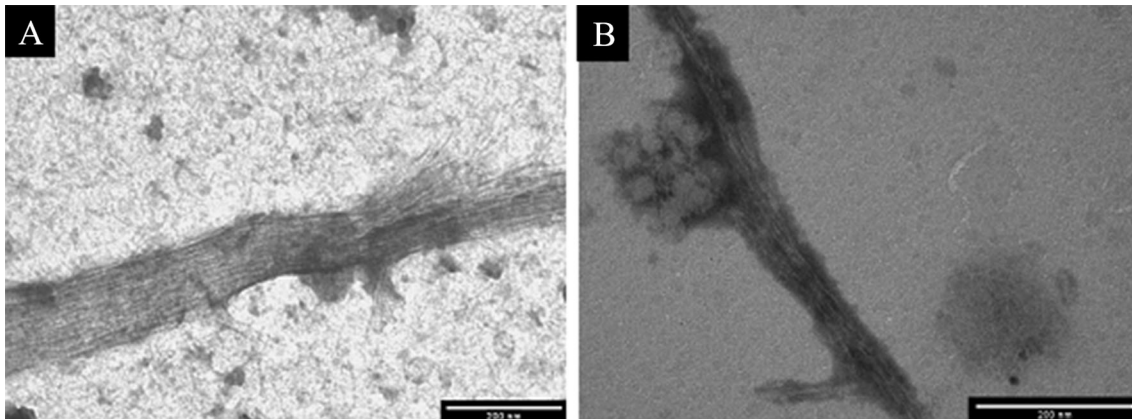


**FIG. 4** Comparison of the amyloidogenic potential of chemically synthesized amylin (A) and carboxy-amy (B) by TEM. Disaggregated peptide samples were prepared in 10 mM sodium phosphate buffer, pH 7.4, containing 50 mM NaCl to a final concentration of 30 M. Representative micrographs of each sample are shown after an incubation time of 60 Min at 37 °C. Scale bars represent 200 nm.

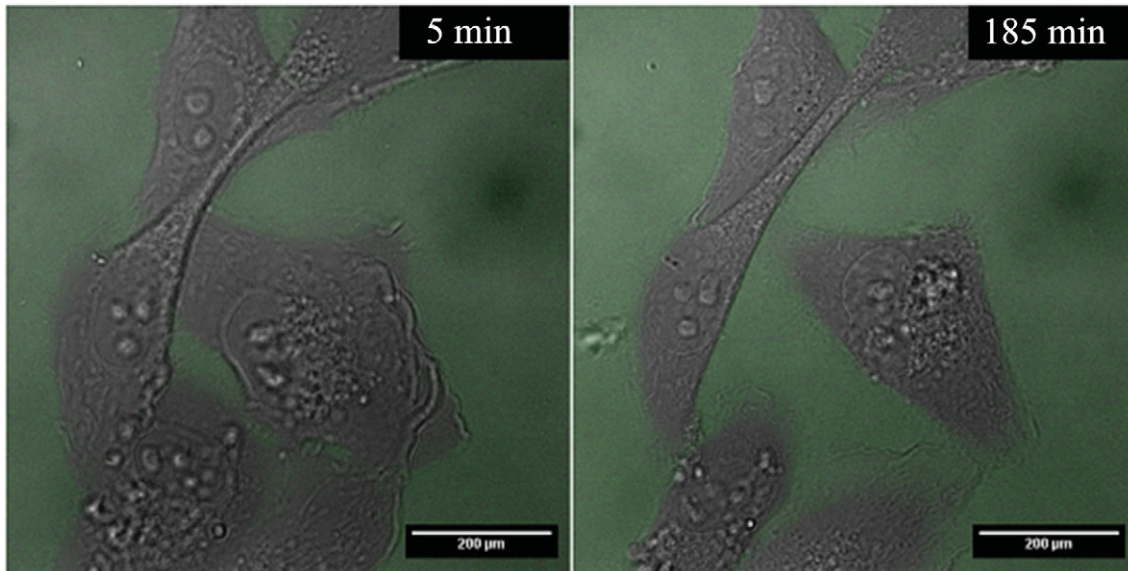


**FIG. 5**

*Confocal microscopy of RIN-5F cells exposed to carboxyfluorescein only (2.54  $\mu\text{M}$ , equivalent to the amount of carboxyfluorescein present in 30  $\mu\text{M}$  of carboxy-amy) at the start of the experiment and after 3 H. The mean fluorescence intensity at 5 Min is  $14.5 \pm 3.0$  and at 185 Min is  $14.2 \pm 3.0$ . The fluorescence intensity of carboxyfluorescein at the two time intervals was observed to be statistically similar ( $P > 0.05$ ). It is thus evident that the carboxyfluorescein label does not undergo photobleaching and neither does it interact with the cells. Each image represents the equatorial region of the cells and is an overlay of the green fluorescent channel and the simultaneously obtained DIC image. Scale bars represent 200  $\mu\text{m}$ . Statistical analysis (Welch's unpaired *t*-test) was performed using GraphPad InStat version 3 (GraphPad Software, CA, USA).*

strategies that are compromised by nonspecific binding interactions and interference of amylin–amylin interactions that precludes reliable data interpretation. The present study was initiated in an attempt to visualize the *in vitro* interaction of amylin aggregates with a cultured mammalian cell line using a confocal microscopy-based fluorescence approach.

To negate any possibility of incorrect data interpretation, it was deemed critical that control experiments using only carboxyfluorescein be performed and the amyloidogenic nature of carboxy-amy be compared with unmodified amylin. In control confocal microscopy experiments using only carboxyfluorescein, it was observed that the fluorophore does not interact with the cells and neither does it aggregate over the duration of the experiment. This was further substantiated by NTA of samples containing carboxyfluorescein only as no particles were detected at all time points. It is thus noteworthy that all observations on carboxy-amy reported in this study represent the modified peptide and are not due to interactions resulting from the carboxyfluorescein tag alone. In addition, carboxy-

amy was shown via TEM analysis to form typical amyloid fibrils that were comparable to those formed by unmodified amylin. It can thus be suggested that attachment of the fluorophore did not impact negatively on the amyloidogenic nature of amylin. This notion is supported by a previous study that reported that the presence of a fluorescein label at the N-terminal of full-length amylin had no significant effect on the amyloidogenic properties of amylin [21]. Thus, it may be suggested that the fluorescent labeling approach as employed in the current study be considered as a viable option to investigate the aggregation dynamics of amylin.

Confocal microscopy imaging resolved that carboxy-amy aggregates specifically interact with the cell membrane of RIN-5F cells. It was also interesting to note that the interactions were limited to certain regions of the membrane as opposed to a more global interactive pattern. As mentioned previously, the carboxy-amy aggregates in certain instances remained strongly associated with the membrane, whereas it shifted during cellular morphological changes. The latter observation is suggestive of a physical interaction between the two entities. This is supportive of previous studies, which found that amylin associates with synthetic membranes, GUVs, or cell membranes [33, 36–39, 41–43, 57, 58]. Possible reasons for amylin interacting with the cell membrane have previously been proposed, with studies suggesting that either hydrophobic or electrostatic interactions are responsible for this association [36–39, 41–43, 57, 58]. Hydrophobic interactions are possible as amylin has more hydrophobic R-groups in its constituent amino acids than hydrophilic R-groups, thus allowing amylin to interact with the nonpolar membranes, whereas electrostatic interactions between positively charged amino acids and the negatively charged membrane could also facilitate amylin-membrane association. For more details on the role of membrane interaction with amyloidogenic peptides and the subsequent, refer to reviews by Stefani [59, 60]. Amylin has also been shown to bind to heparin sulfate proteoglycans that

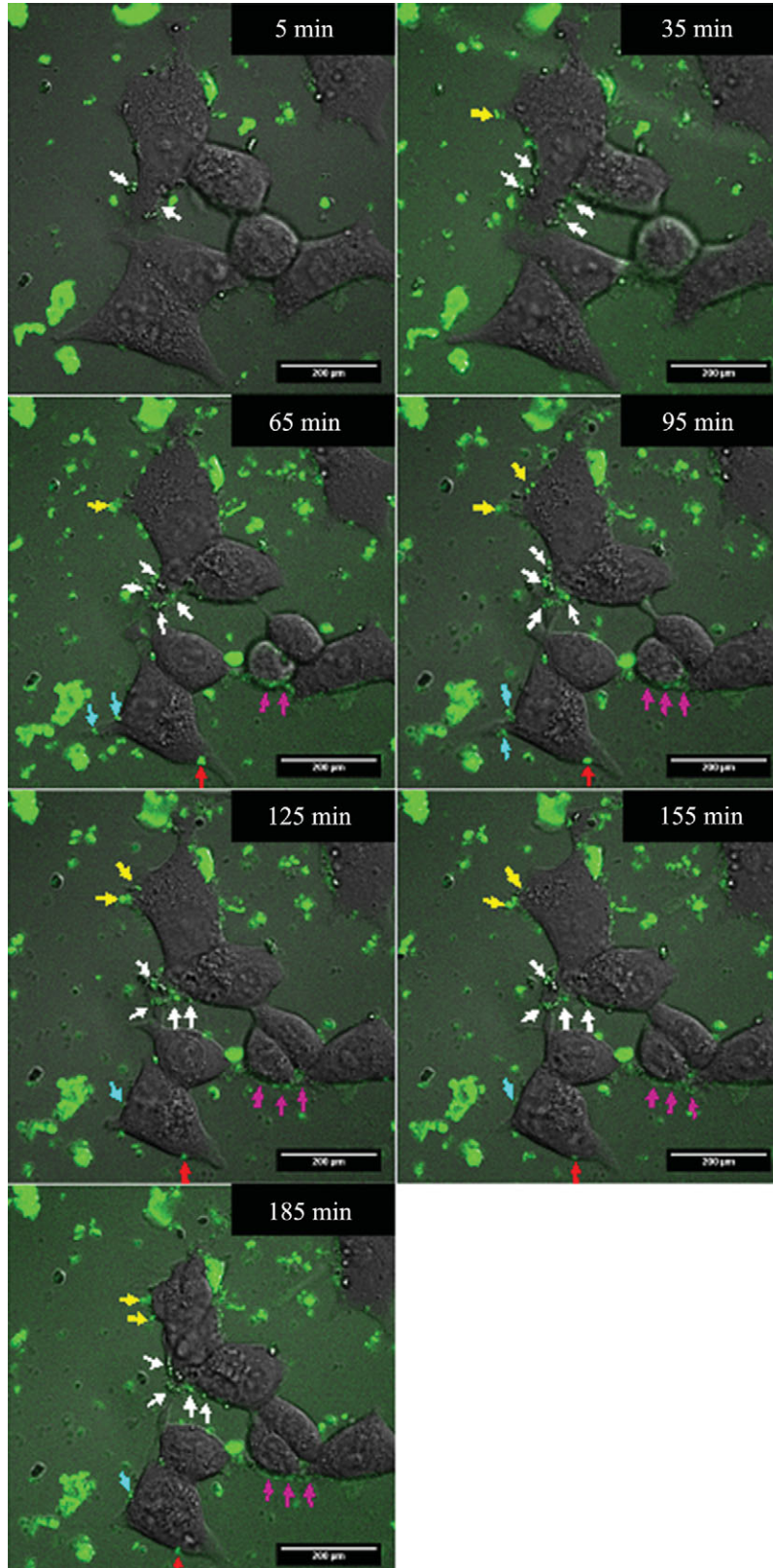


**FIG. 6**

*Carboxy-amy interaction with the cell membrane of RIN-5F cells at 30 Min intervals as determined by confocal microscopy. Each image represents the equatorial region of the cells and is an overlay of the green fluorescent channel and the simultaneously obtained DIC image. Colored arrows are used to indicate the cellular localization of amylin over time. Scale bars represent 200 μm.*

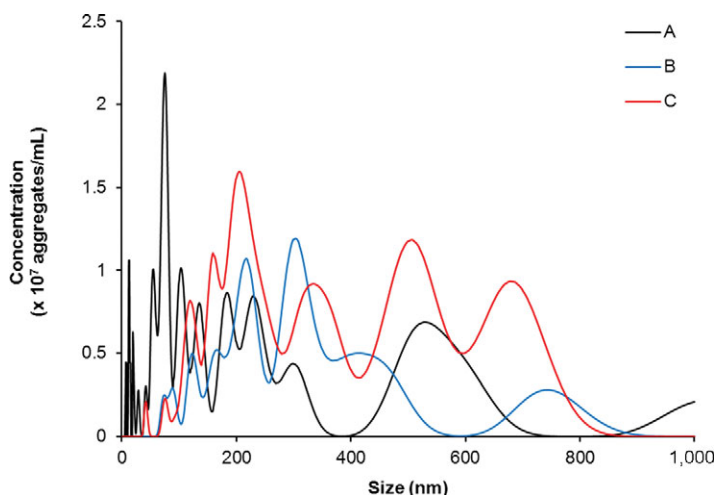


**FIG. 7**

*NTA size distribution profile of disaggregated carboxy-amy (30  $\mu$ M) in 10 mM sodium phosphate buffer, pH 7.4 containing 50 mM NaCl after incubation at 37 °C for 10 Min (A) and 180 Min (B). (C) NTA size distribution profile of the carboxy-amy sample that was recovered from the completed confocal microscopy experiments. Video recordings (duration of 60 Sec) of each sample were taken for NTA using the single shutter and gain mode.*

are present in the basement membrane of pancreatic *beta* cells. The latter binding interaction could also apply to the interaction of carboxy-amy aggregates with RIN-5F cells in this study [61].

Understanding the fine details of the interaction of amylin aggregates with cellular membranes has the potential to unravel the mechanism of amylin-induced cytotoxicity. One hypothesis supported by experimental findings is that amylin mediates cytotoxicity by binding to and initiating pore formation in cellular membranes, thus compromising its integrity [7,8,62]. Another possible amyloidogenic protein-mediated mechanism is that the protein monomer or oligomer would interact with the lipid bilayer of the cell membrane and extract lipids from the membrane during the aggregation process, thereby resulting in membrane damage [41]. This is especially significant as it was reported that a high fat intake or change in lipid metabolism was necessary for fibril formation [63, 64]. A subsequent report suggested that the latter events would result in type II diabetes [36]. In addition, examination of islets revealed that membranes in close proximity to the amyloid deposits appeared to be damaged, which could disrupt membrane fluidity and affect the uptake of glucose by the pancreatic *beta* cells, thereby leading to apoptosis [35]. It was also previously reported that amylin embeds itself in the basement membrane, forming an envelope around the intraislet capillary endothelium, which may have a negative effect on absorption of nutrients and hence could facilitate apoptosis [34]. A more recent study has

also shown that amylin interacts with and damages synthetic membranes of GUVs [43].

Carboxy-amy aggregation was also followed over time using NTA and it was observed that the concentration and size of aggregates increases over the 3 H duration of the experiment. NTA also illustrated that the size distribution profiles of aggregates present in the samples recovered from the confocal microscopy experiment were similar to those of freshly prepared samples. However, it was noted that the concentration of aggregates in the sample recovered from the confocal microscopy experiment was higher than the concentration of aggregates that formed in the carboxy-amy sample that was not exposed to cellular interaction. This finding is similar to that reported by Jayasinghe and Langen [37], who also noted that amylin aggregates much more rapidly in the presence of synthetic membranes containing phosphatidylserine. In the presence of RIN-5F cells, the predominant size ranges of amylin aggregates that were formed were observed to be 130–270, 270–400, 400–600, and 600–800 nm. These data are consistent with a previous study that used total internal reflection fluorescence microscopy and reported that amylin aggregates spanned a size range between 200 and 560 nm [65].

## 5. Conclusion

This study has demonstrated for the first time that labeling of full-length human amylin with the fluorescent tag carboxyfluorescein does not alter the aggregating potential of the peptide. Thus, it can be suggested that this fluorescently labeled peptide could be used to monitor the aggregation dynamics of amylin and hence for screening potential inhibitors of amylin aggregation and possibly even inhibitors of amylin-mediated cytotoxicity. In addition, it was demonstrated that amylin interacts with the cell membrane, which supports the already proposed hypothesis that amylin-mediated cytotoxicity results from membrane disruption.

## 6. Acknowledgements

The authors extend their sincere gratitude to Ms. Celia Snyman, UKZN, for technical advice on use of the confocal microscope and their heartfelt thanks to Dr. James Wesley-Smith, UKZN/CSIR, for expert insight during TEM analysis. Karen Pillay would like to thank the National Research Foundation (NRF) Thuthuka programme (grant number 76066) and UKZN for funding this study.

## 7. References

- [1] Opie, E. (1901) *J. Exp. Med.* 5, 528–540.
- [2] Cooper, G. J. S., Willis, A. C., Clark, A., Turner, R. C., Sim, R. B., and Reid, K. B. M. (1987) *Proc. Natl. Acad. Sci. USA* 84, 8628–8632.
- [3] Cooper, G. J. S., Leighton, B., Dimitriadis, G. D., Parry-Billings, M., Kowalchuk, J. M., Howland, K., Rothbard, J. B., Willis, A. C., and Reid, K. B. M. (1988) *Proc. Natl. Acad. Sci. USA* 85, 7763–7766.
- [4] Kaye, R., Bernhagen, J., Greenfield, N., Sweimeh, K., Brunner, H., Voelter, W., and Kapurniotu, A. (1999) *J. Mol. Biol.* 287, 781–796.



- [5] Pawlicki, S., Le Behec, A., and Delamarche, C. (2008) *BMC Bioinform.* 9.
- [6] Clark, A., Edwards, C. A., Ostle, L. R., Sutton, R., Rothbard, J. B., Morris, J. F., and Turner, R. C. (1989) *Cell Tissue Res.* 257(1), 179–185.
- [7] Janson, J., Ashley, R. H., Harrison, D., McIntyre, S., and Butler, P. C. (1999) *Diabetes* 48, 491–498.
- [8] Anguiano, M., Nowak, R. J., and Lansbury, P. T. (2002) *Biochemistry* 41, 11338–11343.
- [9] Kaye, R., Sokolov, Y., Edmonds, B., McIntire, T. M., Milton, S. C., Hall, J. E., and Glabe, G. C. (2004) *J. Biol. Chem.* 279, 46363–46366.
- [10] Konarkowska, B., et al. (2006) *FEBS J.* 273(15), 3614–3624.
- [11] Meier, J. J., Kaye, R., Lin, C., Gurlo, T., Haataja, L., Jayasinghe, S., Langen, R., Glabe, G. C., and Butler, P. C. (2006) *Am. J. Physiol. Endocrinol. Metab.* 291, E1317–E1324.
- [12] Ritzel, R. A., Meier, J. J., Lin, C., Veldhuis, J. D., and Butler, P. C. (2007) *Diabetes* 56, 65–71.
- [13] Aitken, J. F., Loomes, K. M., Scott, D. W., Reddy, S., Phillips, A. R. J., Prijic, G., Fernando, C., Zhang, S. P., Broadhurst, R., L'Huillier, P., and Cooper, G. J. S. (2010) *Diabetes* 59(1), 161–171.
- [14] Hayashi, T., Asai, T., and Ogoshi, H. (1997) *Tetrahedron Lett.* 38(17), 3039–3042.
- [15] Tomiyama, T., Kaneko, H., Kataoka, K., Asano, S., and Endo, N. (1997) *Biochem. J.* 322, 859–865.
- [16] Rijkers, D. T. S., Hoppener, J. W. M., Posthuma, G., Lips, C. J. M., and Liskamp, R. M. J. (2002) *Chem. Eur. J.* 8(18), 4285–4291.
- [17] Scrocchi, L. A., Chen, Y., Waschuk, S., Wang, F., Cheung, S., Darabie, A. A., McLaurin, J., and Fraser, P. E. (2002) *J. Mol. Biol.* 318, 697–706.
- [18] Aitken, J. F., Loomes, K. M., Konarkowska, B., and Cooper, G. J. S. (2003) *Biochem. J.* 374, 779–784.
- [19] Scrocchi, L. A., Ha, K., Chen, Y., Wu, L., Wang, F., and Fraser, P. E. (2003) *J. Struct. Biol.* 141(3), 218–227.
- [20] Porat, Y., Mazor, Y., Efrat, S., and Gazit, E. (2004) *Biochemistry* 43(45), 14454–14462.
- [21] Taterek-Nossol, M., Yan, L., Schmauder, A., Tenidis, K., Westermarck, G., and Kapurniotu, A. (2005) *Chem. Biol.* 12, 797–809.
- [22] Yan, L., Taterek-Nossol, M., Velkova, A., Kazantzis, A., and Kapurniotu, A. (2006) *Proc. Natl. Acad. Sci. USA* 103(7), 2046–2051.
- [23] Abedini, A., Meng, F., and Raleigh, D. P. (2007) *J. Am. Chem. Soc.* 129, 11300–11301.
- [24] Bedrood, S., Jayasinghe, S., Sieburth, D., Chen, M., Erbel, S., Butler, P. C., Langen, R., and Ritzel, R. A. (2009) *Biochemistry* 48(44), 10568–10576.
- [25] Cabaleiro-Lago, C., Lynch, I., Dawson, K. A., and Linse, S. (2009) *Langmuir* 26(5), 3453–3461.
- [26] Mishra, R., Sellin, D., Radovan, D., Gohlke, A., and Winter, R. (2009) *Chembiochem* 10(3), 445–449.
- [27] Potter, K. J., Scrocchi, L. A., Warnock, G. L., Ao, Z., Younker, M. A., Rosenberg, L., Lipsett, M., Verchere, C. B., and Fraser, P. E. (2009) *Biochim. Biophys. Acta* 1790(6), 566–574.
- [28] Zraika, S., Hull, R. L., Udayasankar, J., Aston-Mourney, K., Subramanian, S. L., Kisilevsky, R., Szarek, W. A., and Kahn, S. E. (2009) *Diabetologia* 52(4), 626–635.
- [29] Meng, F., Abedini, A., Plesner, A., Middleton, C., Potter, K. J., Zanni, M. T., Verchere, C. B., and Raleigh, D. P. (2010) *J. Mol. Biol.* 400(3), 555–566.
- [30] Muthusamy, K., Arvidsson, P. I., Govender, P., Kruger, H. G., Maguire, G. E. M., and Govender, T. (2010) *Bioorg. Med. Chem. Lett.* 20(4), 1360–1362.
- [31] Rigacci, S., Guidotti, V., Bucciattini, M., Parri, M., Nediani, C., Cerbai, E., Stefani, M., and Berti, A. (2010) *J. Nutr. Biochem.* 21(8), 726–735.
- [32] Doig, A. J., Stott, K., and Treherne, J. M. (2004) *Biotechnol. Genet. Eng. Rev.* 21, 197–212.
- [33] Verchere, C. B., Dalessio, D. A., Palmiter, R. D., Weir, G. C., Bonner-Weir, S., Baskin, D. G., and Kahn, S. E. (1996) *Proc. Natl. Acad. Sci. USA* 93(8), 3492–3496.
- [34] Hayden, M. R., and Tyagi, S. C. (2001) *J. Pancreas* 2(4): 124–39.
- [35] Clark, A., and Nilsson, M. R. (2004) *Diabetologia* 47(2), 157–169.
- [36] Knight, J. D., and Miranker, A. D. (2004) *J. Mol. Biol.* 341(5), 1175–1187.
- [37] Jayasinghe, S. A., and Langen, R. (2005) *Biochemistry* 44, 12113–12119.
- [38] Engel, M. F. M., Yigittop, H., Elgersma, R. C., Rijkers, D. T. S., Liskamp, R. M. J., de Kruijff, B., Hoppener, J. W. M., and Killian, J. A. (2006) *J. Mol. Biol.* 356(3), 783–789.
- [39] Apostolidou, M., Jayasinghe, S. A., and Langen, R. (2008) *J. Biol. Chem.* 283(25), 17205–17210.
- [40] Hiddinga, H. J., and Eberhardt, N. L. (1999) *Am. J. Pathol.* 154(4), 1077–1088.
- [41] Sparr, E., Engel, M. F. M., Sakharov, D. V., Sprong, M., Jacobs, J., de Kruijff, B., Hoppener, J. W. M., and Killian, J. A. (2004) *FEBS Lett.* 577(1–2), 117–120.
- [42] Radovan, D., Opitz, N., and Winter, R. (2009) *FEBS Lett.* 583(9), 1439–1445.
- [43] Khemtemourian, L., Domenech, E., Doux, J. P. F., Koorengel, M. C., and Killian, J. A. (2011) *J. Am. Chem. Soc.* 133(39), 15598–15604.
- [44] Cooper, J. H. (1974) *Lab. Invest.* 31(3), 232–238.
- [45] Lansbury, P. T. (1992) *Biochemistry* 31(30), 6865–6870.
- [46] Padrick, S. B., and Miranker, A. D. (2001) *J. Mol. Biol.* 308(4), 783–794.
- [47] Jaikaran, E., Nilsson, M. R., and Clark, A. (2004) *Biochem. J.* 377, 709–716.
- [48] Yan, L., Velkova, A., Taterek-Nossol, M., Andreetto, E., and Kapurniotu, A. (2007) *Angew. Chem. Int. Ed.* 46, 1246–1252.
- [49] Knight, J. D., Williamson, J. A., and Miranker, A. D. (2008) *Protein Sci.* 17(10), 1850–1856.
- [50] Marek, P., Gupta, R., and Raleigh, D. P. (2008) *ChemBioChem* 9(9), 1372–1374.
- [51] Fulop, L., Penke, B., and Zarandi, M. (2001) *J. Pept. Sci.* 7(8), 397–401.
- [52] Muthusamy, K., Albericio, F., Arvidsson, P. I., Govender, P., Kruger, H. G., Maguire, G. E. M., and Govender, T. (2010) *Biopolymers* 94(3), 323–330.
- [53] Edwin, N. J., Bantchev, G. B., Russo, P. S., Hammer, R. P., and McCarley, R. L. (2005) *KorugicKarasz, L. S., MacKnight, W. J., and Martuscelli, E., Editors. New Polymeric Materials.* pp. 106–118.
- [54] Edwin, N. J., Hammer, R. P., McCarley, R. L., and Russo, P. S. (2010) *Biomacromolecules* 11(2), 341–347.
- [55] Goncalves, M. S. T. (2009) *Chem. Rev.* 109(1), 190–212.
- [56] Filipe, V., Howe, A., and Jiskoot, W. (2010) *Pharm. Res.* 27(5), 796–810.
- [57] Lopes, D. H. J., Meister, A., Gohlke, A., Hauser, A., Blume, A., and Winter, R. (2007) *Biophys. J.* 93(9), 3132–3141.
- [58] Radovan, D., Smirnovas, V., and Winter, R. (2008) *Biochemistry* 47(24), 6352–6360.
- [59] Stefani, M. (2007) *Neuroscientist* 13(5), 519–531.
- [60] Stefani, M. (2010) *FEBS J.* 277(22), 4602–4613.
- [61] Marzban, L., Park, K., and Verchere, C. B. (2003) *Exp. Gerontol.* 38(4), 347–351.
- [62] Mirzabekov, T. A., Lin, M., and Kagan, B. L. (1996) *J. Biol. Chem.* 271, 1988–1992.
- [63] Hoppener, J. W. M., Oosterwijk, C., Nieuwenhuis, M. G., Posthuma, G., Thijssen, J. H. H., Vroom, T. M., Ahren, B., and Lips, C. J. M. (1999) *Diabetologia* 42(4), 427–434.
- [64] Hull, R. L., Andrikopoulos, S., Verchere, C. B., Vidal, J., Wang, F., Cnop, M., Prigeon, R. L., and Kahn, S. E. (2003) *Diabetes* 52(2), 372–379.
- [65] Patil, S. M., Mehta, A., Jha, S., and Alexandrescu, A. T. (2011) *Biochemistry* 50(14), 2808–2819.